Bibliography

Abbot, I. and von Doenhoff, A. (1959) *Theory of Wing Sections*, Dover Publications, Second edition.

Agenbag, D. (2000) "Development of a design real time pitch flight simulator for the Exulans glider", Final year thesis, Department of Mechanical and Aeronautical Engineering, University of Pretoria, RSA.

Althaus, D. and Wortmann, F. (1981) *Stuttgarter Profilkatalog I*, Vieweg, Braunschweig/Wiesbaden.

Anonymous (1997) "Human factors for designers of equipment. part 2: Body size.", Defence Standard DEF STAN 00-25 (Part 2)/Issue 2, British Ministry of Defence, UK.

Anonymous (2005) "Echoing to the sound of silence", *Aerospace Testing International, September issue*.

Anonymous (2006) "Göppingen Gö 3", Website, `http://en.wikipedia.org`, Accessed 19 December 2006.

Anonymous (n.d. a) "Flying wing history", Website, `www.yourzagi.com`, Accessed 19 May 2004.

Anonymous (n.d. b) "The flying wings of Charles Fauvel", Website, `http://www.nurflugel.com/Nurflugel/Fauvel/e_biograph.htm`, Accessed 4 May 2001.

Anonymous (n.d. c) "Goldfields gliding club homepage", Website, `www.ggc.co.za`, Accessed 27 October 2004.

Anonymous (n.d. d) "Jim Markse flying wings pioneer photo gallery", Website, `http://www.continuo.com/marske/pioneer/photogal.htm`, Accessed 4 May 2001.

Anonymous (n.d. e) "SZD 20 Wampir 2", Website, `http://www.vintagesailplanes.de/SZD_20.htm`, Accessed 19 May 2004.

Anonymous (n.d. f) "Nietoperz", Website, `http://www.vintagesailplanes.de/nietoper.htm`, Accessed 19 May 2004.

Anonymous (n.d. g) "Northrop flying wing", Website, `http://www.pilotfriend.com/century-of-flight/Aviation`, Accessed 19 May 2004.

Anonymous (n.d. h) "Pyxis", Website, `http://users.skynet.be/nestofdragons/pyxis.htm`, Accessed 18 June 2004.

Anonymous (n.d. i) "Rigid-wing models - The Flair 30", Website, `http://midtoad.homelinux.org/midwinter.ca/RigidWings/flair30.htm`, Accessed 25 May 2004.

Anonymous (n.d. j) "Schleicher ASW-19", Website, `http://www.gliding-in-melbourne.org/asw19.htm`, Accessed 19 January 2005.

Ashkenas, I. and Klyde, D. March (1989) "Tailless aircraft performance improvements with relaxed static stability", Contractor Report CR-181806, NASA, USA.

Browne, K. (2003) "The instrumentation and initial analysis of the short-term control and stability derivatives of an ASK-13 glider.", Master's thesis, Department of Electronic Engineering, University of Stellenbosch, Stellenbosch, RSA.

Bryan, G. (1911) *Stability in Aviation*, Macmillan, London.

Calise, A.; Lee, S. and Sharma, M. (2000) "Development of a reconfigurable flight control law for the X-36 tailless fighter aircraft", Conference paper, AIAA Guidance, Navigation, and Control Conference, 14-17 August, 2000/Denver, CO.

Chalk, C. (1963) "Fixed-base simulator investigation of the effects of L_α and true speed on pilot opinion of longitudinal flying qualities", Technical Documentary Report ASD-TDR-63-399, Flight Dynamics Laboratory Research and Technology Division Air Force Systems Command, Wright-Patterson Air Force Base, Ohio.

Chun, H. H. and Chang, C. H. (2001) "Longitudinal stability and dynamic motions of a small passenger WIG craft", *Ocean Engineering,* (29), 1145–1162.

Cooper, G. and Harper, R. (1969) "The use of pilot rating in the evaluation of aircraft handling qualities", Technical Note D5153, NASA, USA.

Cronje, J. (1999) "Pitch flight simulator for the Exulans 2, final year thesis report", University of Pretoria, RSA.

Crosby, C. P. (1997) *Strategies for Glider Performance Improvement*, PhD thesis, Department of Mechanical and Aeronautical Engineering, University of Pretoria, RSA.

Crosby, C. P. (2000) "Aerodynamic coefficients for the Exulans 2 glider", Personal communication.

Dods, J. (1948) "Wind-tunnel investigation of horisontal tails. Part III - unswept and 35° swept-back plan forms of aspect ratio 6", Report RM A8H30, NACA, USA.

Drela, M. and Youngren, H. (2000) *XFoil 6.9 User Primer*, Department of Aeronautical and Astronautical Engineering, MIT, Boston, USA, Last updated edition.

Etkin, B. (1972) *Dynamics of Atmospheric Flight*, John Wiley & Sons, Inc., New York.

Fremaux, C. and Vairo, D. (1995) "Effect of geometry and mass distribution on tumbling characteristics of flying wings", *AIAA Journal of Aircraft, 32* (2).

Holly, P. (2005) "Under surveillance - the Boeing ScanEagle", *Aerospace Testing International, September issue.*

Horstmann, K. and Shürmeyer, C. (1985) "Development of airfoil sections for the swept-back tailless sailplane SB 13", Conference paper, Rieti, Italy.

Horstmann, K.-H. (1988) "Ein Mehrfach-Traglinienverfahren un seine Verwendung für Entwurf und Nachrechnen nichtplanarer Flügelanordnungen. (A multiple lifting line method and its application for the design and calculation of non-planar wing configurations.)", Forschungsbericht DFVLR-FB 87-51, DFVLR, Braunschweig.

Huyssen, R. J. (2000) "Mass properties of the Exulans 2 glider", Personal communication.

Huyssen, R. (1994) "Investigation into the feasibility of a new concept of ultra light hang glider", Master's thesis, Department of Mechanical and Aeronautical Engineering, University of Pretoria, RSA.

Kay, J.; Mason, W. H.; Durham, W.; Lutze, F. and Benoliel, A. (1996) *Control Authority Issues in Aircraft Conceptual Design: Critical Conditions, Estimation Methodology, Spreadsheet Assessment, Trim and Bibliography*, Department of Aerospace and Ocean Engineering, Virginia Polytechnic Institute and State University, Blacksburg, Virginia 24061, Unpublished edition.

Kroo, I. (2000) "Design and development of the SWIFT: A foot-launched sailplane", *AIAA Journal of Aircraft,* (AIAA-00-4336).

Kroo, I.; Beckman, E.; Robbins, B.; Morris, S. and Porter, B. (1991) "Development of the SWIFT - A tailless foot-launched sailplane", Website, `http://aero.stanford.edu/Reports/SWIFTArticle1991.html`, Accessed 4 May 2001.

Kuethe, A. M. and Chow, C. (1998) *Foundations of Aerodynamics - Bases of Aerodynamic Design*, John Wiley and Sons inc., USA.

McCormick, B. W. (1995) *Aerodynamics, Aeronautics and Flight Mechanics*, John Wiley and Sons inc., USA.

Melin, T. (2001) *Tornado 1.0 User's Guide Reference Manual*, Royal Institute of Technology (KTH), Department of Aeronautics, Sweden, Release 2.3 edition.

MIL-F-8785C (1980) "MIL Specification F8785C, Flying qualities of piloted airplanes", U.S. Department of Defense Military Specification.

Moes, T. and Iliff, K. (2002) "Stability and control estimation flight test results for the SR-71 aircraft with externally mounted experiments", Report TP-2002-210718, NASA, USA.

Mönnich, W. and Dalldorff, L. (1993) "A new flying qualities criterion for flying wings", *AIAA Journal of Aircraft,* (AIAA PAPER 93-3668).

Neal, T. and Smith, R. (1970) "An in-flight investigation to develop control system design criteria for fighter airplanes", *AFFDL-TR-70-74, Air Force Flight Dynamics Laboratory, Wright-Patterson AFB, Ohio, I and II.*

Nickel, K. and Wohlfahrt, M. (1994) *Tailless aircraft in theory and practice*, Edward Arnold, London first edition.

O'Hara, F. (1967) "Handling criteria", *Journal of the Royal Aeronautical Society, 71* (676), 271–291.

Park, M. (2000) "Steady-state computation of constant rotational rate dynamic stability derivatives", *AIAA Journal of Aircraft,* (AIAA 2000-4321).

Roskam, J. (1971) *Methods for Estimating Stability and Control Derivatives of Conventional Subsonic Airplanes*, The University of Kansas, Lawrence, Kansas, USA, First edition.

Shomber, H. and Gertsen, W. (1967) "Longitudinal handling qualities criteria: An evaluation", *Journal of Aircraft, 4* (4), 371–376.

Stevens, B. L. and Lewis, F. L. (1992) *Aircraft Control and Simulation*, John Wiley and Sons inc., USA.

Thomas, F. (1993) *Fundamentals of Sailplane Design*, College Park Press, College Park Maryland, USA.

Tobie, H.; Elliot, E. and Malcom, L. (1966) "A new longitudinal handling qualities criterion", Conference paper, National Aerospace Electronics Conference, Dayton, Ohio.

Toll, T. and Queijo, M. (1948) "Approximate relations and charts for low-speed stability derivatives of swept wings", Technical Note TN-1581, NACA, USA.

Wilson, J. (2003) "Battle of the X-Planes", *Popular Mechanics RSA, June edition.*

Zientek, A. (1992) "A polish flying experience with tailless gliders.", *Technical Soaring, 16* (2), 48–56.

Index

Appendix A

The Cooper-Harper Scale

The following table presents the Cooper-Harper scale that is used to express pilot rating (PR) of aircraft handling qualities.

Table A.1: Pilot opinion rating and flying qualities level. (The Cooper Harper scale)

Aircraft characteristics	Demands on pilot in selected task or required operation	Pilot rating	Flying qualities level
Excellent; highly desirable	Pilot compensation not a factor for desired performance	1	
Good; negligible deficiencies	Pilot compensation not a factor for desired performance	2	1
Fair; mildly unpleasant deficiencies	Minimal pilot compensation required for desired performance	3	
Minor but annoying deficiencies	Desired performance requires moderate pilot compensation	4	
Moderately objectionable deficiencies	Adequate performance requires considerable pilot compensation	5	2
Very objectionable but tolerable deficiencies	Adequate performance requires extensive pilot compensation	6	
Major deficiencies	Adequate performance not attainable with maximum tolerable pilot compensation. Controllability not in question	7	
Major deficiencies	Considerable pilot compensation required for control	8	3
Major deficiencies	Intense pilot compensation required to retain control	9	
Major deficiencies	Control will be lost during some portion of required operation	10	

Appendix B

Eigenvalue Analysis

Eigenvalue analysis of a mechanical system requires a mathematical description of the system dynamics. An aircraft can be modelled by means of the equations of motion just like any other mechanical system. It has inertial properties like mass and moment of inertia. It also has damping properties represented by the aerodynamic damping coefficients. It has properties that have similar characteristics to the stiffness of a spring that obeys Hooke's law. An example of a 'stiffness' is the lift force that has a linear dependence on the angle of attack (α).

The equations used to describe aircraft dynamics can be expressed in the following matrix form:

$$m\ddot{\overline{x}} + c\dot{\overline{x}} + k\overline{x} = \overline{F} \tag{B.1}$$

The variable $\overline{F}$ in this equation represents a column vector of external excitation forces and moments. In the case of the aircraft this represents forces and moments from the control surfaces. The control surfaces are controlled by the pilot of the aircraft. The velocity column vector is now defined as

$$\overline{y} = \dot{\overline{x}} \tag{B.2}$$

Equation B.2 can now be substituted into Equation B.1 in order to yield another form of the matrix equation:

$$m\dot{\overline{y}} + c\overline{y} + k\overline{x} = \overline{F} \tag{B.3}$$

Equations B.2 and B.3 are now combined:

$$\begin{bmatrix} m & 0 \\ 0 & I \end{bmatrix} \begin{bmatrix} \dot{\overline{y}} \\ \dot{\overline{x}} \end{bmatrix} + \begin{bmatrix} c & k \\ -I & 0 \end{bmatrix} \begin{bmatrix} \overline{y} \\ \overline{x} \end{bmatrix} = \begin{bmatrix} \overline{F} \\ 0 \end{bmatrix} \tag{B.4}$$

For the eigenvalue (modal) analysis that we want to perform, the inherent dynamics of the mechanical system have to be analysed. This means that the forced excitation $\overline{F}$ is set equal to zero before the eigenvalue analysis is performed. Having done this, Equation B.4 is rewritten and the following state space representation of the aircraft model follows:

$$\begin{bmatrix} \dot{y} \\ \dot{x} \end{bmatrix} = - \begin{bmatrix} m & 0 \\ 0 & I \end{bmatrix}^{-1} \begin{bmatrix} c & k \\ -I & 0 \end{bmatrix} \begin{bmatrix} y \\ x \end{bmatrix} \tag{B.5}$$

The state space representation is now of the form:

$$\dot{z} = Az \tag{B.6}$$

with

$$z = \begin{bmatrix} x^T & y^T \end{bmatrix}^T \tag{B.7}$$

where

$$A = - \begin{bmatrix} m & 0 \\ 0 & I \end{bmatrix}^{-1} \begin{bmatrix} c & k \\ -I & 0 \end{bmatrix} \tag{B.8}$$

The eigenvalues of matrix A are used to calculate the natural frequencies and damping ratios of the natural modes of the system.

The resulting eigenvalues are in real or conjugate pairs. Each complex conjugate pair can be associated with a natural oscillation mode and can be expressed in a form analogous to a single degree of freedom system, where ζ_r is the damping ratio and ω_r is the circular natural frequency corresponding to the r-th eigenvalue of the system:

$$s_r = -\zeta_r \omega_r + i\omega_r \sqrt{1-\zeta_r^2} \tag{B.9}$$

$$s_r^* = -\zeta_r \omega_r - i\omega_r \sqrt{1-\zeta_r^2} \tag{B.10}$$

The damped natural frequency is calculated with Equation B.11.

$$\omega_{d_r} = \omega_r \sqrt{1-\zeta_r^2} \tag{B.11}$$

The damped natural frequencies are important parameters in analysing the dynamics of a multi degree of freedom system.

The aircraft rigid body equations of motion are non-linear. Eigenvalue analysis require a set of linear differential equations. It is important to note that the matrix A of Equation B.6 may be considered as the coefficient matrix of a linearised version of the non-linear aircraft equations of motion at a particular aircraft flight regime or trim state.

Appendix C

Aircraft Planforms in this Study

The following aircraft planforms were part of the handling quality investigation.

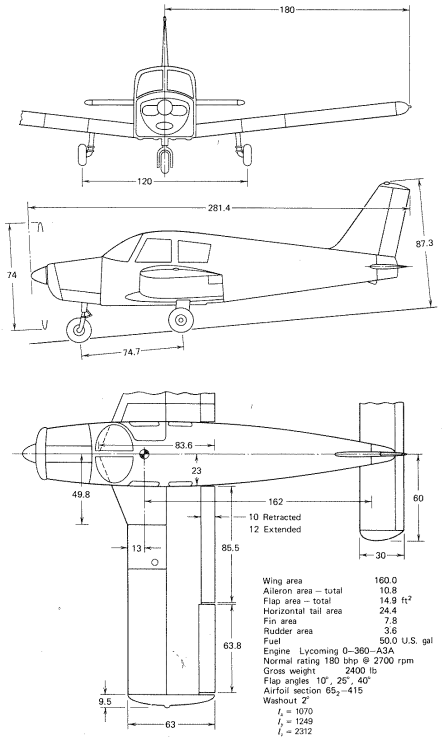

(a) Piper Cherokee PA-28-180 aircraft, all dimensions in inches (McCormick, 1995:123).

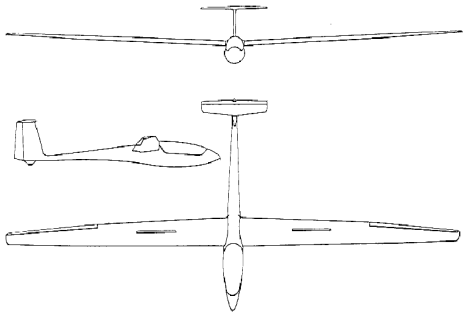

(b) The ASW-19 aircraft (Anonymous, n.d. j).

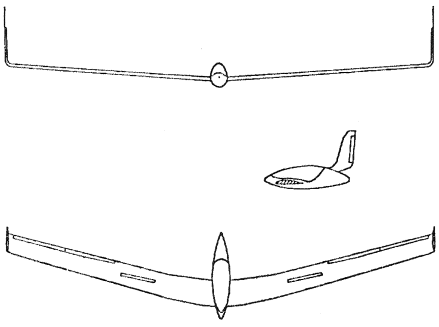

(c) The SB-13 aircraft (Mönnich & Dalldorff, 1993:448).

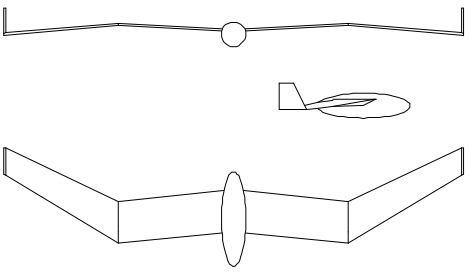

(d) The gull-wing configuration (30° sweep-back angle).

Figure C.1: Planforms that formed part of the handling quality investigation.

Appendix D

Time Step Size

Time domain simulations of aircraft dynamic responses were executed using a Runge Kutta fourth order method. This method was also used in Stevens & Lewis (1992). The effect of the time step size on the convergence of the simulation response was investigated by means of comparative simulations. This was done in order to optimise the time step size with respect to both convergence of the response and simulation execution time. The investigation revealed that simulations with a 0.01 second time step size yielded sufficiently converged time domain responses.

Figures D.1 to D.6 shows simulation results for four different time step sizes (0.1, 0.01, 0.001 and 0.0001 seconds). The simulation results show the gust response of an Exulans with 30° wing sweep and a static margin layout of 10.7% at 30°. A cosine gust model (with the same magnitude as described in Section 4.8.1) was used as the disturbance.

The results show that time step size has the largest influence on attitude and true airspeed response. Figure D.3 shows the effect of time step on the short period attitude response. This simulation result shows that a 0.01 second time step size calculates the attitude response with sufficient convergence.

A time step size of 0.01 seconds was consequently used for all simulations that are presented in this study.

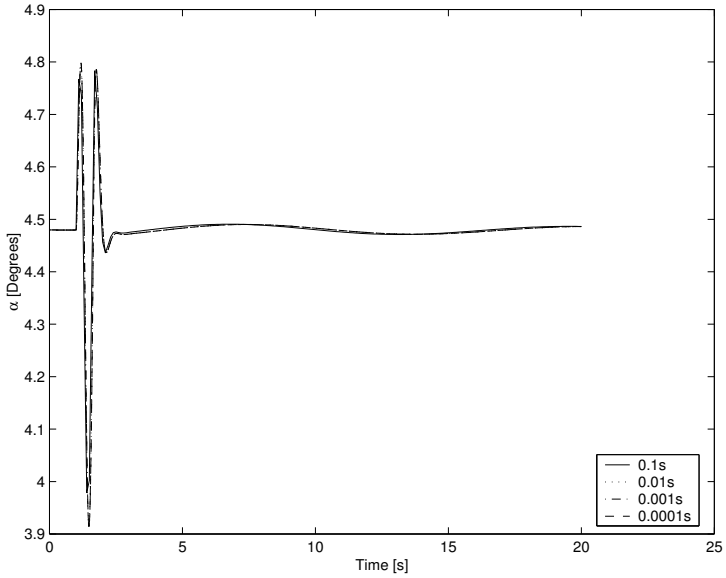

Figure D.1: The effect of step size on angle of attack (α) response for four step sizes.

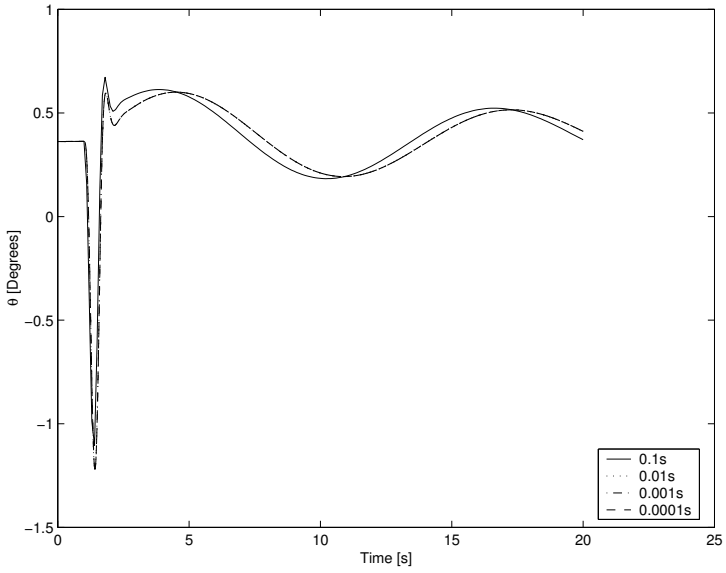

Figure D.2: The effect of step size on attitude (θ) response for four step sizes.

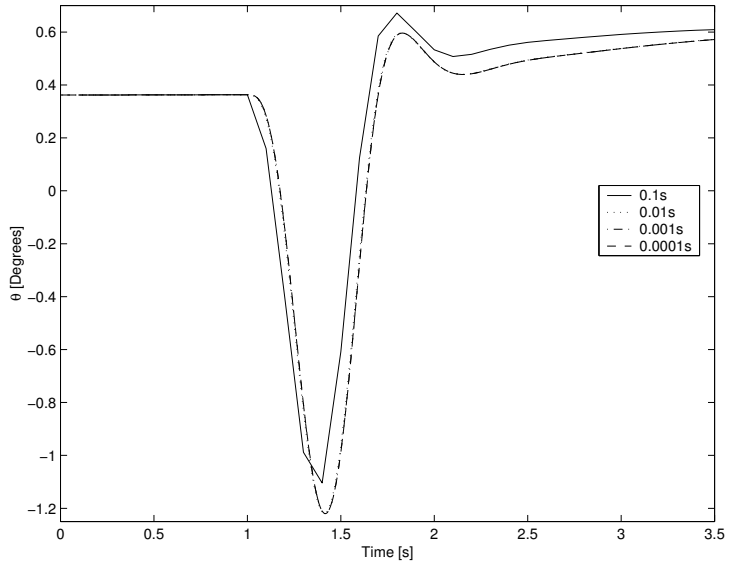

Figure D.3: The effect of step size on the short period attitude (θ) response for four step sizes (Zoomed-in portion of Figure D.2).

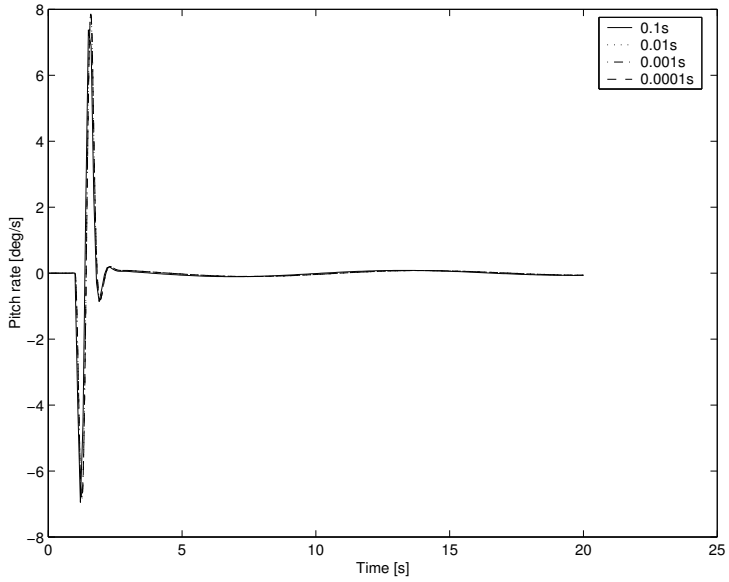

Figure D.4: The effect of step size on the pitch rate response for four step sizes.

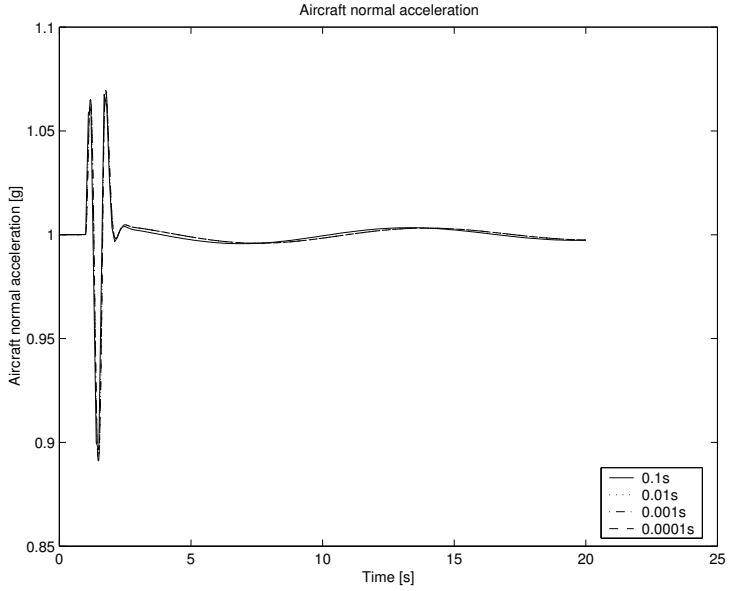

Figure D.5: The effect of step size on the normal acceleration response for four step sizes.

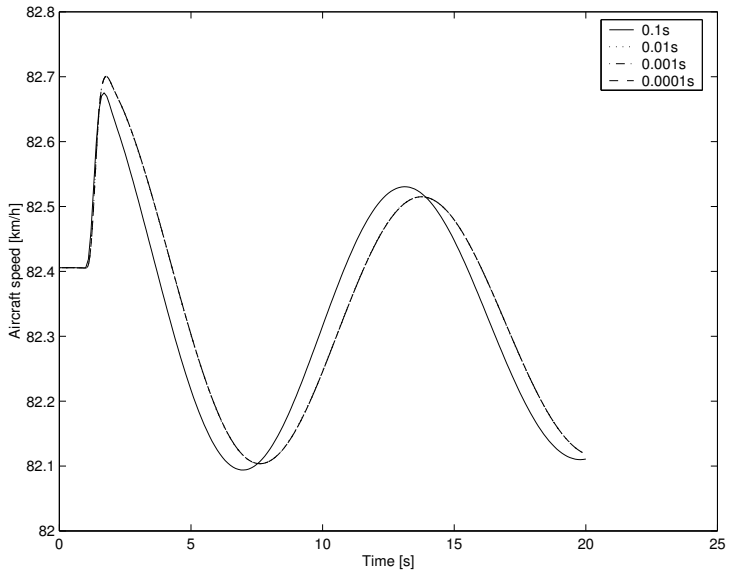

Figure D.6: The effect of step size on the true airspeed response for four step sizes.

Appendix E

C_{M_q} Benchmark Investigation

The damping coefficient (C_{M_q}) is an important parameter when calculating the natural frequencies and damping ratios of the phugoid and short period motions. It is therefore necessary to calculate or measure it accurately before using the damping coefficient values in calculations.

Damping coefficients can be obtained through wind tunnel measurements, numerical methods such as CFD or vortex lattice methods, or by means of system identification methods from measurements in real flight.

The vortex lattice method was chosen as the method with which to numerically estimate aircraft damping coefficients for the purpose of this study. It was chosen since this type of method is suitable for calculating the damping coefficients of complex planform geometries, while being less computationally intensive than Navier Stokes fluid dynamic numerical methods.

Since the calculation accuracy of the damping coefficient is important to this study, it was necessary to determine the level of accuracy of the vortex lattice method codes that were used in this study. Two different vortex lattice codes, namely JKVLM[1] and Tornado were used in this study.

The accuracy of the two vortex lattice methods was evaluated by means of comparison with the wind tunnel results of damping coefficients for four different wing planforms that are presented in Toll & Queijo (1948:52).

[1] J. Kay Vortex Lattice Method

E.1 Planforms under Investigation

The damping coefficients of the four different wing planforms of Toll & Queijo (1948:47) were calculated using the JKVLM and Tornado vortex lattice method implementations.

The wing planforms that were used in the investigation are presented in Figure E.1.

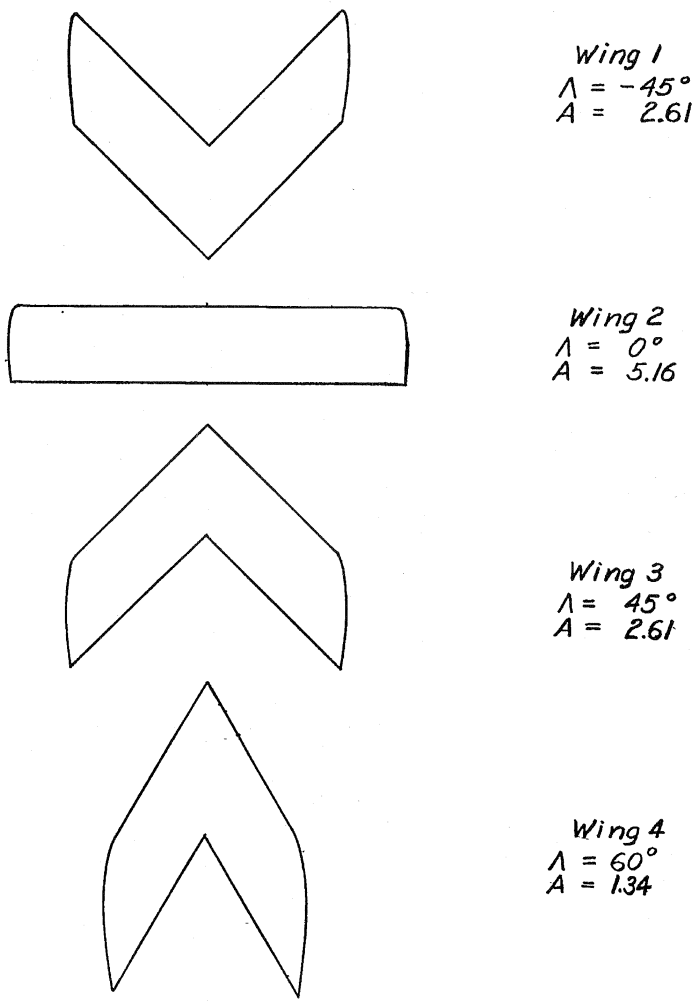

Figure E.1: The four wing planform types used in the vortex lattice method benchmark study. (Toll & Queijo, 1948:47)

E.2 Results and Conclusions

A sensitivity study of the value of C_{M_q} with respect to the number of elements on the wing was performed using the Tornado vortex lattice method. The results of this study are shown in Figure E.2. Inspection of this figure shows that convergence is reached with a relatively small number of elements.

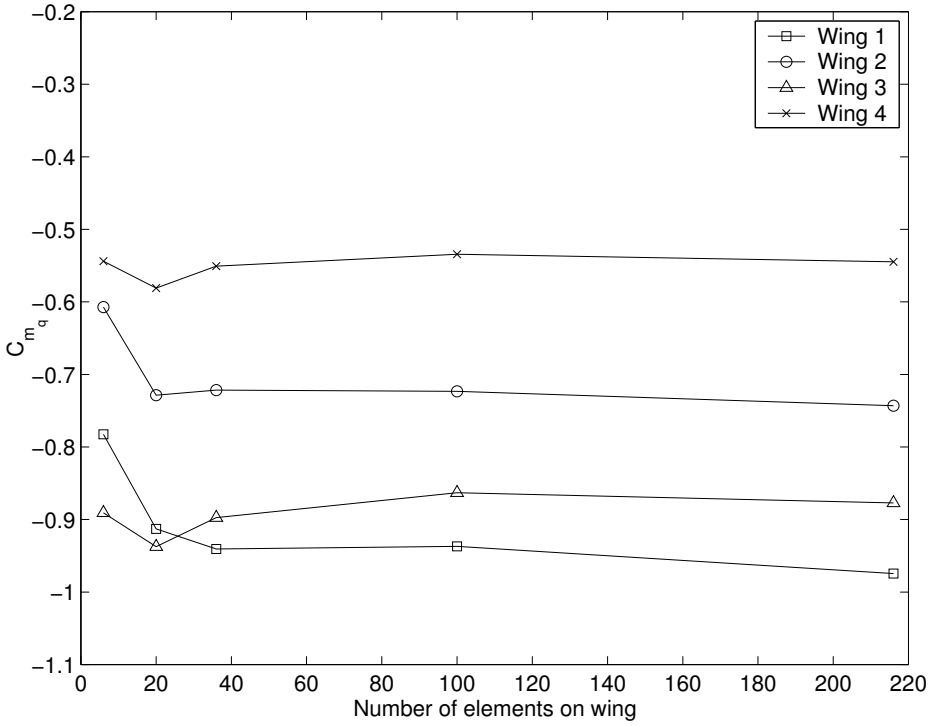

Figure E.2: Convergence of C_{M_q} values as calculated with the Tornado vortex lattice method.

The results of the benchmark study are shown in Figure E.3. The results are also presented in table format in Table E.1. The results of the two vortex lattice methods show good agreement with each other. The vortex lattice method results and wind tunnel results do not show very good agreement for C_{M_q} values (see results of Wing 2, Figure E.3), but are of the same order of magnitude. The results of the benchmark study indicate that poor results for C_{M_q} are obtained when a straight wing planform is analysed. Large discrepancies between experimental and calculated results for highly swept

wings at moderate and high lift coefficients are most likely caused by partial separation of flow which results in changes in the distributions of lift and drag along the wing span (Toll & Queijo, 1948:27). The gull-wing configuration is a combination of a forward swept and a backward swept wing. The vortex lattice method showed acceptable accuracy (within 20% for moderate lift coefficients) for these wing types. The damping coefficient resulting from the vortex lattice method is constant across the whole range of lift coefficients shown, as it is a linear method.

The value of C_{M_q} that is labelled as 'Calculated' in Figure E.3 and Table E.1 was obtained using Equation E.1 (Toll & Queijo, 1948:25)[2]. This equation can be used to calculate C_{M_q} for swept wings. The results show that the vortex lattice methods show very good agreement with this analytical approximation.

$$C_{M_q} = -a_0 \cos\Lambda \left\{ \frac{\chi\left[2\left(\frac{\overline{X}}{\overline{c}}\right)^2 + \frac{1}{2}\frac{\overline{X}}{\overline{c}}\right]}{\chi + 2\cos\Lambda} + \frac{1}{24}\frac{\chi^3 \tan^2\Lambda}{\chi + 6\cos\Lambda} + \frac{1}{8} \right\} \tag{E.1}$$

Table E.1: Comparison of values of C_{M_q} calculated by different methods

Wing number	Calculated	JKVLM	Tornado
1	-0.935	-0.939	-0.975
2	-0.709	-0.764	-0.743
3	-0.935	-0.951	-0.877
4	-0.551	-0.593	-0.545

The damping coefficient values calculated for the Exulans were used as inputs to a handling quality study. The baseline damping coefficient values (as calculated by vortex lattice methods) were varied by 20% above and below the baseline. This was done since the estimation error is roughly 20% above and below the baseline damping ratio. By varying the damping in this manner the effect of the estimation error on handling qualities can be

[2]Equation 50 in that document.

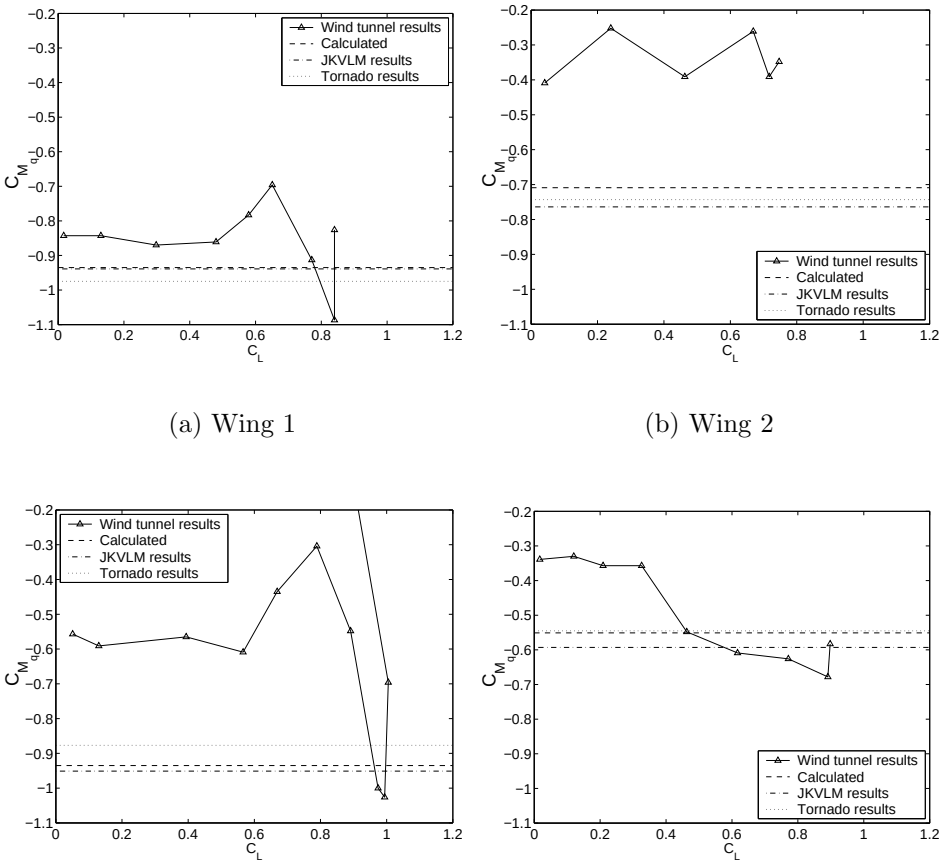

(a) Wing 1

(b) Wing 2

(c) Wing 3

(d) Wing 4

Figure E.3: C_{M_q} values for different angles of attack from experimental data (Toll & Queijo, 1948:58) compared with calculated values from vortex lattice methods.

determined. The aerodynamic damping was varied by 50% (as a worst case scenario) during the gull-wing sensitivity analysis to gauge the sensitivity of the handling qualities to such a large variation in damping.

Since the uncertainty in the damping coefficient was estimated, the uncertainty in the handling qualities analysis results resulting from this estimation error can be quantified. The handling qualities of the aircraft can therefore be determined to be within a certain band. The handling qualities can be judged to be acceptable or marginal by evaluating this band. This is sufficient for a preliminary handling quality analysis where a prototype aircraft is not yet available to measure handling qualities accurately by means of flight testing.

It is therefore concluded that the vortex lattice methods codes that are used in this study have the capability to calculate damping coefficients of swept wing aircraft with sufficient accuracy for handling qualities analysis.

Appendix F

$C_{M_{\delta e}}$ Benchmark Investigation

The accuracy with which the vortex lattice method, JKVLM, can predict the moment control surface derivative, $C_{M_{\delta_e}}$, was determined. $C_{M_{\delta_e}}$ is the aerodynamic moment resulting from elevon deflection. The ratio of $C_{M_{\delta_e}}$ to $C_{L_{\delta_e}}$ is important with respect to handling qualities for a tailless aircraft, since the elevon deflection on such an aircraft does not produce negligible aerodynamic lift. The aerodynamic lift may lead to an undesirable phenomenon called pancaking. $C_{L_{\delta_e}}$ is calculated with sufficient accuracy by VLM's, but not $C_{M_{\delta_e}}$.

This section presents JKVLM calculations that were used to determine the $C_{M_{\delta_e}}$ parameter for an elevator. An unswept elevator and a 35° swept-back elevator were analysed. The results were compared with wind tunnel results (see Dods (1948)) to determine the accuracy of the VLM predictions.

F.1 Planforms under Investigation

Two elevators having different planform characteristics (see Figure F.1) were used in the benchmark investigation. An unswept planform and one with a 35° sweep-back were used.

The models used to obtain the wind tunnel data for the different plan forms both had the NACA 64A010 airfoil. This is a symmetrical airfoil. The two planforms were modelled by flat plate panels in the vortex lattice models.

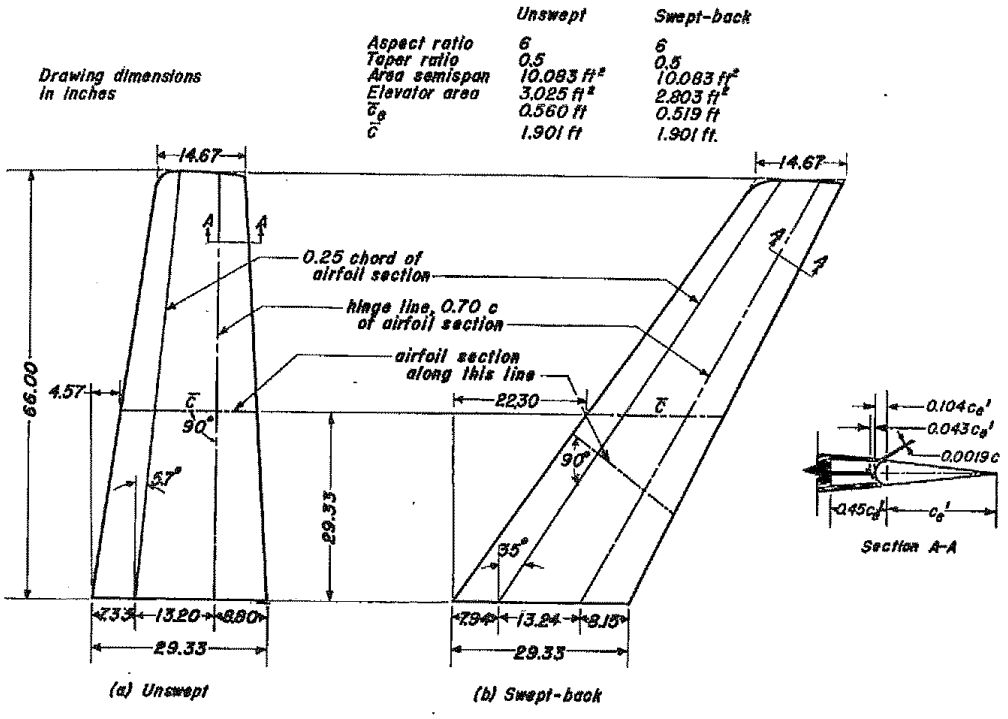

Figure F.1: Planforms of the horizontal tail models of aspect ratio 6 used in the benchmark investigation. (Dods, 1948:13)

F.2 Wind tunnel Data

The empirical lift and moment coefficient data presented in Dods (1948) was used to calculate $C_{M_{\delta_e}}$ for various angles of attack and elevator deflection angles. The wind tunnel data is presented in Figures F.3 to F.6.

The pitching moment coefficients shown in Figures F.4 and F.6 were measured around a lateral axis through a point at 25% the length of the mean aerodynamic chord. The position of the moment reference axis is presented in Figure F.2.

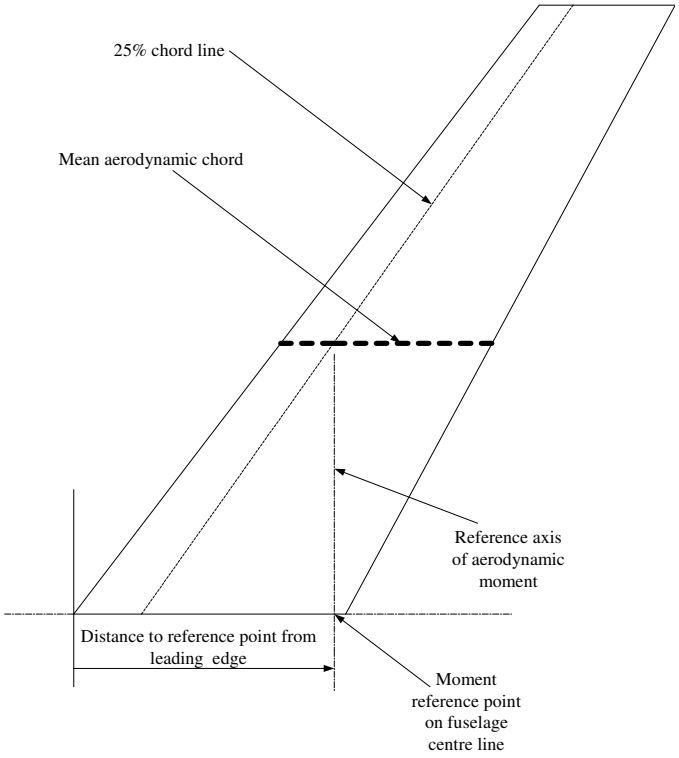

Figure F.2: Aerodynamic moment reference axis as used in Dods (1948:.)

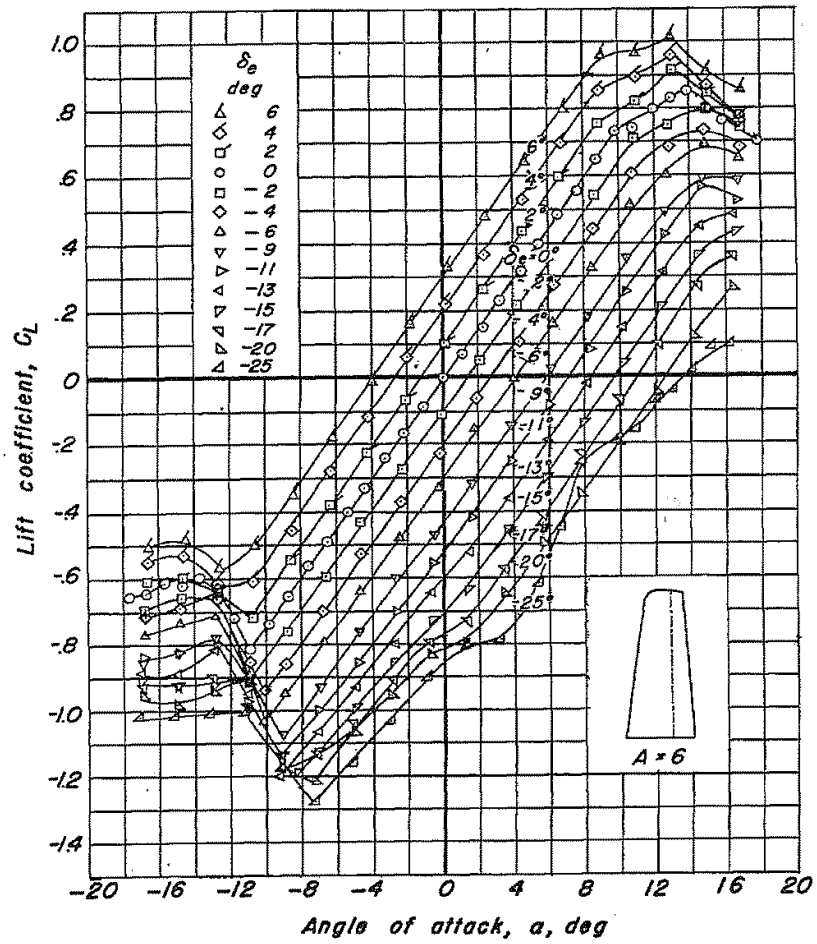

Figure F.3: Lift coefficients of an unswept tail. Aspect ratio, 6; R_e, 3.0×10^6. (Dods, 1948:19)

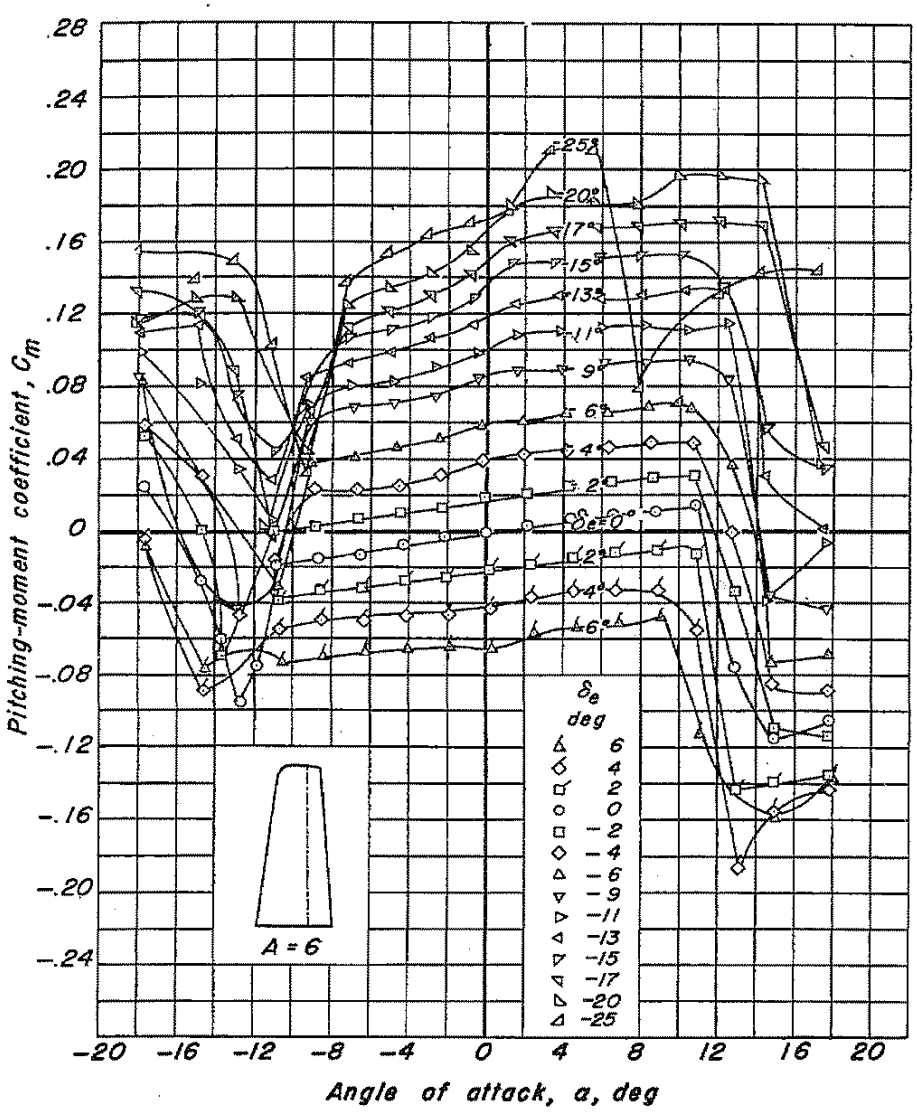

Figure F.4: Pitching moment coefficients of an unswept tail. Aspect ratio, 6; R_e, 3.0×10^6. The moments are measured around a lateral axis through a point that is 25% chordwise aft of the leading edge on the mean aerodynamic chord. (Dods, 1948:21)

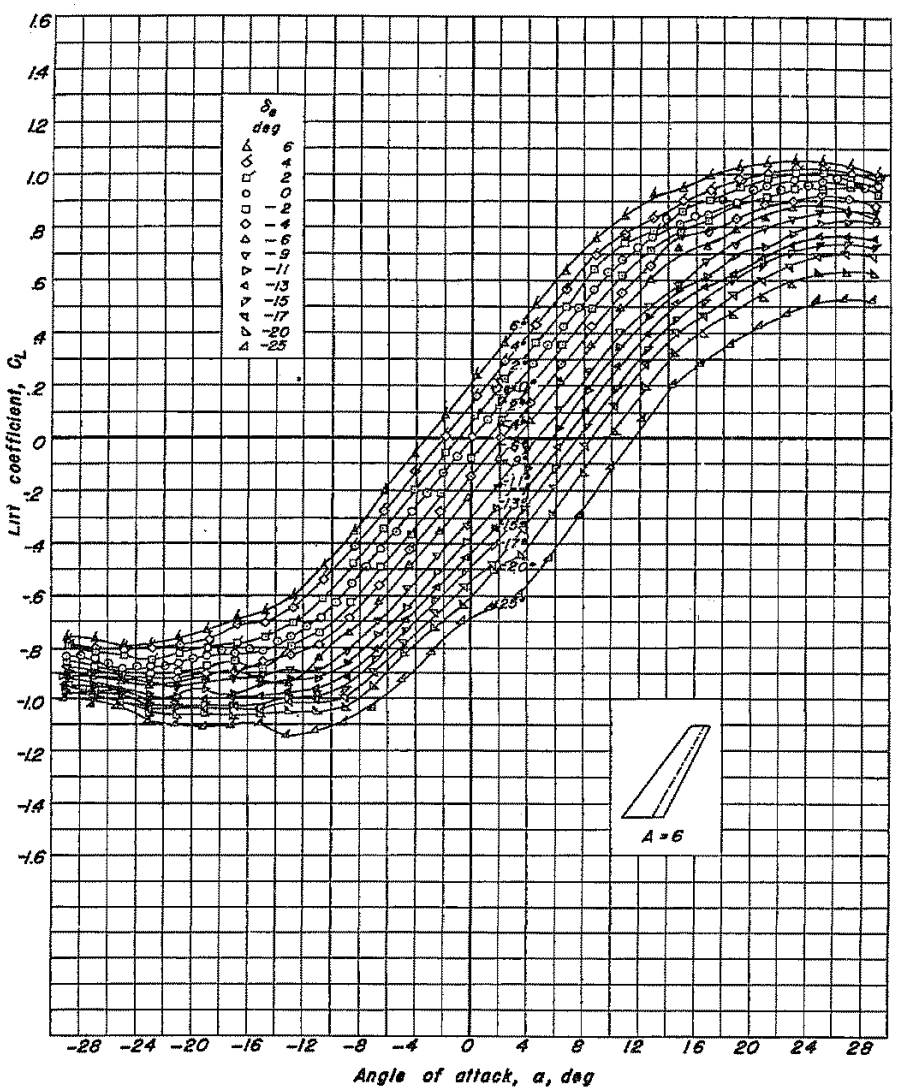

Figure F.5: Lift coefficients of a 35° swept-back tail. Aspect ratio, 6; R_e, 3.0×10^6. (Dods, 1948:29)

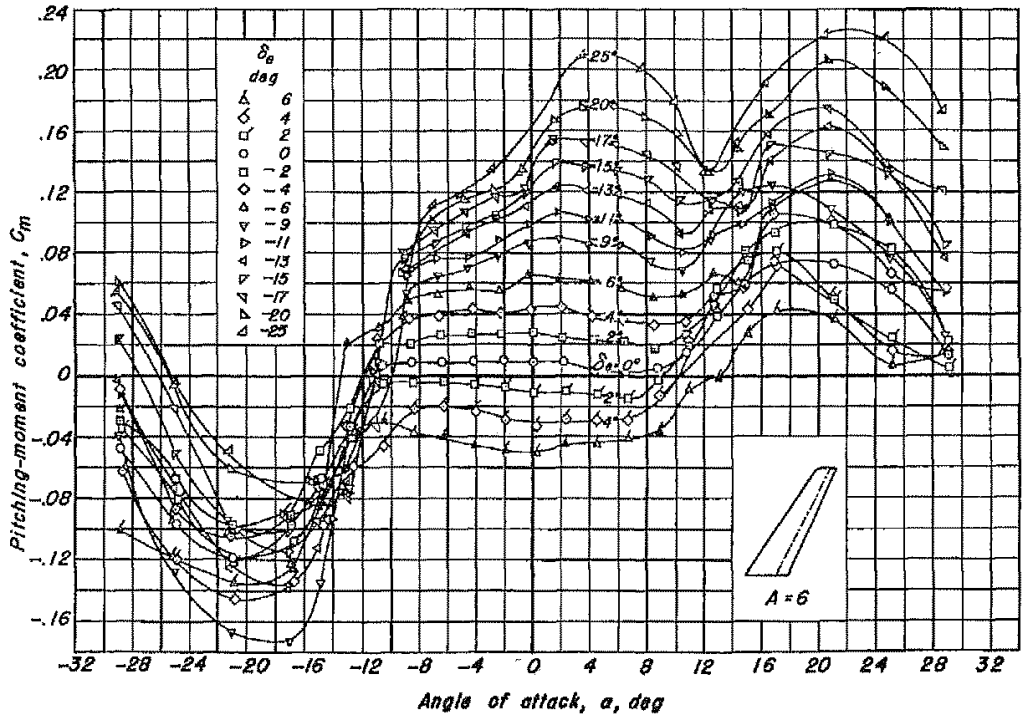

Figure F.6: Pitching moment coefficients of a 35° swept-back tail. Aspect ratio, 6; R_e, 3.0×10^6. The moments are measured around a lateral axis through a point that is 25% chordwise aft of the leading edge on the mean aerodynamic chord. (Dods, 1948:31)

F.3 The Sensitivity of $C_{M_{\delta_e}}$ with respect to Panel Size in VLM's.

A sensitivity study was performed to investigate the influence of the number of elements on the elevon panel on the magnitude of $C_{M_{\delta_e}}$. This parameter can not be adjusted in the JKVLM input file. The analysis was performed using the Tornado vortex lattice method that does have an input parameter for adjusting the number of elements on the elevon.

The sensitivity study was performed using the same elevator wing geometry described in Appendix F.2. Both the swept and unswept wing geometries were used in the sensitivity analysis.

The VLM panel layouts used in the sensitivity analysis are presented in Table F.1. The number of panels were increased on the control panel in order to investigate the effect of more panels on the convergence of the moment coefficient calculation.

Table F.1: VLM model sizes used for the $C_{M_{\delta_e}}$ sensitivity analysis.

Layout	Spanwise elements	Chordwise elements	Chordwise elements on control surface	Total elements
1	10	5	5	100
2	10	5	10	200
3	10	5	15	300
4	20	5	15	400
5	20	10	15	500

The results of the sensitivity study are presented in Figure F.7.

The sensitivity results indicate that the coefficients are already converged at 100 elements. Table F.2 presents JKVLM and Tornado results for the same geometric wing shapes that were used in the sensitivity analysis. The Tornado results are of the same order of magnitude as the JKVLM results. This indicates that the two codes give similar results and that the default number of elements of the JKVLM code produces a result that is sufficiently

converged.

Table F.2: Comparison of the JKVLM elevator deflection coefficients with Tornado results. All coefficients have the units [/rad]

	JKVLM		Tornado	
	Unswept wing	35° swept-back wing	Unswept wing	35° swept-back wing
$\partial C_L/\partial\alpha$	4.649	4.133	4.404	3.9482
$\partial C_M/\partial\alpha$	0.027	-0.167	0.065	-0.057
$\partial C_L/\partial\delta_e$	3.015	2.199	2.941	2.207
$\partial C_M/\partial\delta_e$	-0.634	-0.581	-0.598	-0.565

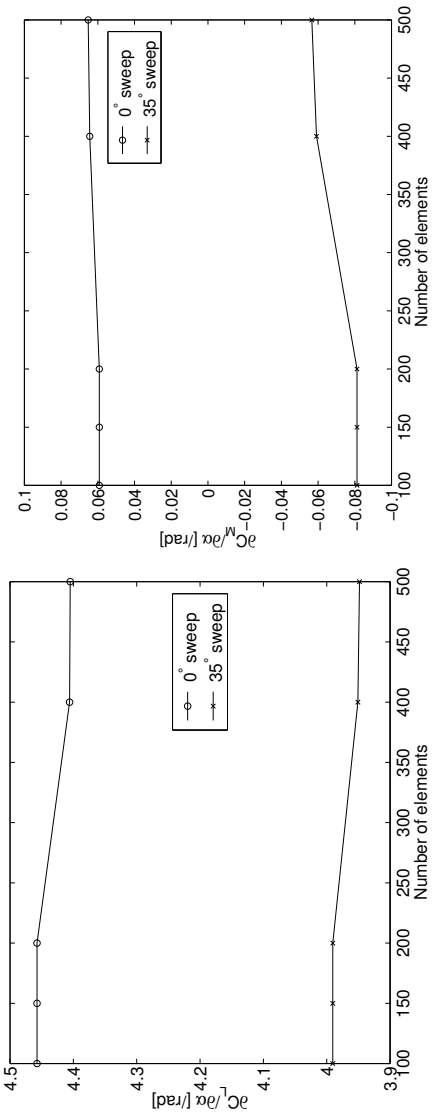

(a) C_{L_α} vs number of elements on wing for 0° and 35° sweep-back wing.

(b) C_{M_α} vs number of elements on wing for 0° and 35° sweep-back wing.

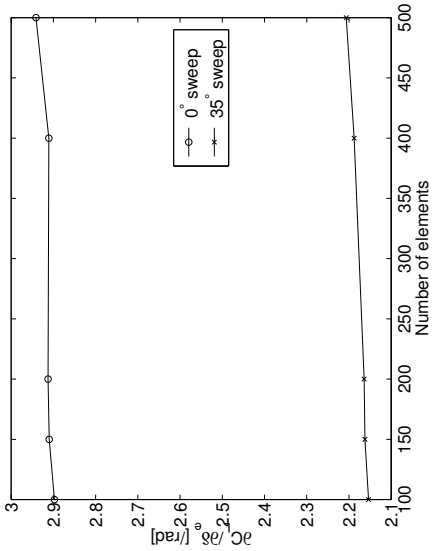

(c) $C_{L_{\delta_e}}$ vs number of elements on wing for 0° and 35° sweep-back wing.

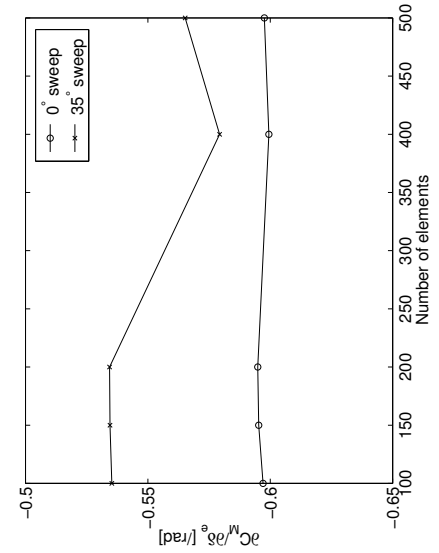

(d) $C_{M_{\delta_e}}$ vs number of elements on wing for 0° and 35° sweep-back wing.

Figure F.7: Sensitivity study with respect to the number of panel elements on the wing for the C_{L_α}, C_{M_α}, $C_{L_{\delta_e}}$ and $C_{M_{\delta_e}}$ parameters.

F.4 Results and Conclusions

The $C_{L_{\delta_e}}$ and $C_{M_{\delta_e}}$ estimates from JKVLM for the two types of elevator are presented in Table F.3. The JKVLM results are compared with wind tunnel results. The wind tunnel results presented in the table are for an angle of attack of 0°. The values of $C_{L_{\delta_e}}$ and $C_{M_{\delta_e}}$) presented in the table are average values for elevator deflections from -5° to 5°.

The reference position for the moment coefficients is around a lateral axis through the same reference point shown in F.2.

Table F.3: Comparison of the calculated elevator deflection coefficients with wind tunnel results for the same coefficients. All coefficients have the units [/rad]

	JKVLM		Wind tunnel	
	Unswept wing	35° swept-back wing	Unswept wing	35° swept-back wing
$\partial C_L/\partial\alpha$	4.649	4.133	4.257	3.581
$\partial C_M/\partial\alpha$	0.027	-0.167	0.082	0.000
$\partial C_L/\partial\delta_e$	3.015	2.199	3.063	1.910
$\partial C_M/\partial\delta_e$	-0.634	-0.581	-0.573	-0.537

The results from the JKVLM calculations for the two types of elevator for $C_{L_{\delta_e}}$ and $C_{M_{\delta_e}}$ are presented in Figure F.8. The JKVLM results are constant over the elevator deflection range. This is because the vortex lattice method is linear.

The following conclusions can be drawn from the results presented here:

- $C_{L_{\delta_e}}$ is predicted with satisfactory accuracy. For elevator deflection angles of -15° to 6° it is valid to treat the value of $C_{L_{\delta_e}}$ as constant. For more negative angles than -15° the value of the parameter cannot be considered constant any more. This can be attributed to viscous effects. This has little impact on the simulations presented in this study, since only small deflections (less than five degrees) are used.

- $C_{M_{\delta_e}}$ is not predicted very accurately by means of the vortex lattice

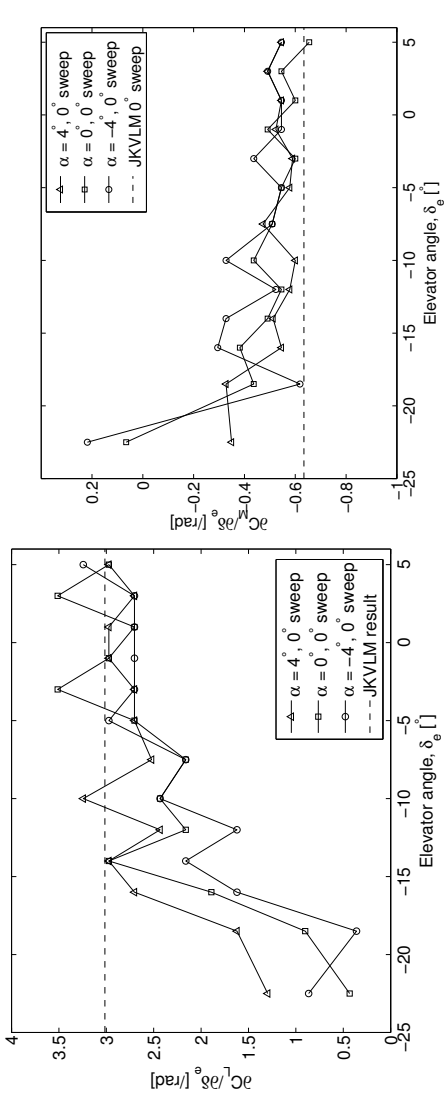

(a) $C_{L_{\delta_e}}$ vs elevator deflection for 0° sweep-back wing.

(b) $C_{M_{\delta_e}}$ vs elevator deflection for 0° sweep-back wing.

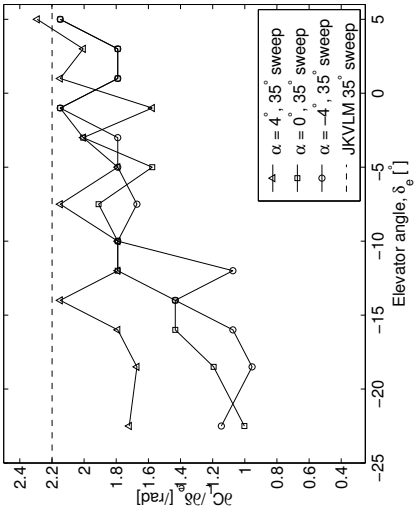

(c) $C_{L_{\delta_e}}$ vs elevator deflection for 35° sweep-back wing.

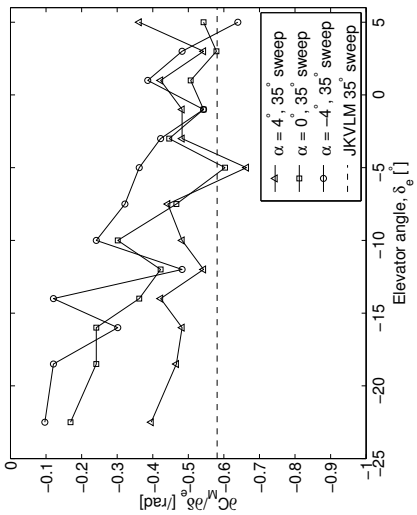

(d) $C_{M_{\delta_e}}$ vs elevator deflection for 35° sweep-back wing.

Figure F.8: Comparison of calculated values of $C_{L_{\delta_e}}$ and $C_{M_{\delta_e}}$ with wind tunnel data.

method. The estimation error is 20% from the vortex lattice baseline result for small angles of attack (less than four degrees) and small deflection angles (less than 5 degrees). This study is limited to small angles of attack and small deflection angles and therefore the estimation error figure of 20% shall be used in determining the sensitivity of the aircraft response to this error.

- C_{M_α} is not predicted accurately by means of the vortex lattice method. The discrepancy of the coefficient is larger for a swept-back wing than for an unswept wing. These errors are attributed to viscous effects and cross-flow that are not modelled in the vortex lattice method.

- As a general trend, prediction errors with respect to $C_{L_{\delta_e}}$, C_{L_α} and C_{M_α} are larger when the wing sweepback angle is larger.

- The accuracy of $C_{L_{\delta_e}}$ of the horizontal tail surface is important for the accurate simulation of the pitch plane dynamics of conventional aircraft with an empennage, while $C_{M_{\delta_e}}$ is more important for the accurate simulation of the pitch plane dynamics of tailless aircraft.

- The accuracy of the estimations of the aerodynamic coefficients is judged to be sufficient for a preliminary handling quality investigation such as the one presented in this work. The estimation error was quantified using the wind tunnel results. The handling qualities can be investigated for a range of the aerodynamic properties (particularly $C_{M_{\delta_e}}$). This range of handling quality results can then be used to determine the sensitivity with respect to the estimation error.

Appendix G

Neutral Point Benchmark Study

The accuracy of the prediction of the neutral point by means of the vortex lattice method was investigated. Wind tunnel results were used to estimate accuracy. The neutral point for two elevator models was calculated using the aerodynamic data presented in Dods (1948). The neutral points of the same two models were estimated using a VLM. The measured and estimated values for the two models are compared and presented here. The numerical convergence of the neutral point calculation with respect to the number of VLM elements used, is also investigated.

G.1 Wind tunnel results

The wind tunnel results used in the benchmark investigation of the moment control surface derivative, $C_{M_{\delta_e}}$, were also used for benchmarking of the neutral point. This data is presented in Appendix F.2. The wind tunnel results relevant to the neutral point are summarised in Table G.1. This table presents the neutral point and static margin for two elevator wind tunnel models. One model has no sweep and the other has 35° wing sweep. The position of the neutral point as presented in Table G.1 is expressed as a percentage of mean aerodynamic chord. The position is given as a distance

aft of the leading edge of the wing on the root chord. This convention is different from and should not be confused with the convention used in Dods (1948). In Dods (1948) the chordwise position on the wing is expressed as a fraction of the mean aerodynamic chord, aft of the leading edge of the wing at the spanwise position where the chord equals the mean aerodynamic chord.

Table G.1: Wind tunnel results for the neutral point. The neutral point position is given in percentage of mean aerodynamic chord.

Parameter	Unswept wing	35° swept-back wing
$\partial C_L/\partial\alpha$ [/rad]	4.257	3.581
$\partial C_M/\partial\alpha$ [/rad]	0.082	0.000
Static margin	-1.92%	0.00%
Neutral point	43.54%	122.90%

The neutral point of Table G.1 corresponds to an approximate position around the quarter chord, calculated at the mean aerodynamic chord. For the swept-back wing this position is significantly further aft of the leading edge at the root chord when compared to the unswept wing.

Table G.1 contains the item 'static margin'. For an aircraft the static margin is determined as the distance between the CG of the aircraft and the neutral point. In the case of the test specimen described here, the axis around which the aerodynamic moment was measured, was used as the chordwise 'CG' of the specimen and the static margin was calculated accordingly. The position of this axis was taken to be the chordwise quarter chord distance aft of the leading edge at that spanwise position where the chord of the test specimen equals the mean aerodynamic chord. This position is where one would expect the neutral point of a symmetrical profile to be. The actual neutral point is not at this position due to three dimensional flow effects.

The values of the neutral point and the static margin of the test specimen as presented in Table G.1 was obtained from the test results presented in Dods (1948).

G.2 Neutral Point Using VLM

The neutral point (and static margin) of the Exulans was estimated by means of a vortex lattice method (VLM). The vortex lattice method was chosen since it is often used to obtain a rapid estimation of aircraft properties while an aircraft is still in the concept phase. For a handling qualities investigation such as the one presented in this document, the fidelity of aircraft properties as calculated by the VLM is sufficient. This is justified by the fact that a general configuration is investigated (albeit with the Exulans as a specific example) and that a sensitivity analysis was performed to gauge the effect of inaccuracies in the aircraft model on predicted handling qualities. The VLM has some disadvantages (see Section G.3) leading to inaccurate predictions, but the accuracy can be quantified (see same Section) and has an acceptable magnitude.

In general a VLM models the wing or lifting surface of the aircraft as a series of closed trapezoidal vortex rings. The actual vortex ring is displaced downstream by a quarter chord of each panel. A control point is located at the center of each ring, where a non-penetration surface boundary condition is imposed. The strengths of each of the vortex rings must be found so that the vector sum of their induced velocity and the free-stream contribution at each control point satisfies the boundary conditions. The induced velocity at a point due to a straight line segment of a vortex filament is given by the Biot-Savart Law. The vortex strengths of the lifting surface panels are represented by a system of simultaneous linear equations. These equations are solved to obtain the vortex strengths. The vortex strengths are integrated over the surface to obtain the aerodynamic forces and moments. Once the moment distribution over the lifting surface is known, the sum of moments may be used to find the point on the lifting surface where the aerodynamic moment is a constant with respect to angle of attack. This point is known as the neutral point of the lifting surface. Kay et al. (1996) may be consulted for a more detailed description of the vortex lattice method theory.

The JKVLM programme was the vortex lattice method used for estimating the neutral point of the gull wing configuration. This programme has

static margin as one of its output parameters. The moment reference point of the aircraft is an input parameter for JKVLM. This point was varied until the calculated static margin was zero. At this point the neutral point coincides with the reference point. This method was also used to calculate the neutral point for the neutral point benchmark study.

The geometry of the wing models of Dods (1948) was entered into the JKVLM programme and the neutral point and static margin of these models were estimated. The results of this effort is presented in Table G.2. The sensitivity of the neutral point value with respect to the number of vortex lattice elements was also investigated. It showed that reasonable convergence was achieved from 120 elements on a wing model (Figure G.1). The position of the moment reference point that was used for the elevator test specimens of Dods (1948) was entered as a CG reference in the vortex lattice method with which the same geometry was analysed. The distance between the neutral point of the elevator geometry analysed with the VLM and this reference point is the static margin value that is presented in Figure G.1.

Table G.2: VLM results for the neutral point. The neutral point position is given in percentage of mean aerodynamic chord.

Parameter	Unswept wing	35° swept-back wing
$\partial C_L/\partial\alpha$ [/rad]	4.494	4.002
$\partial C_M/\partial\alpha$ [/rad]	0.047	-0.085
Static margin	-1.06%	2.13%
Neutral point	44.40%	125.03%

G.3 Wind tunnel and VLM Comparison

The neutral point and static margin from wind tunnel data for the models of Dods (1948) can be compared with the VLM estimates for the same models. The static margin of the wind tunnel elevator specimen was determined by measuring aerodynamic moments around a fixed reference point. The distance of this point to the neutral point of the elevator test specimen is defined

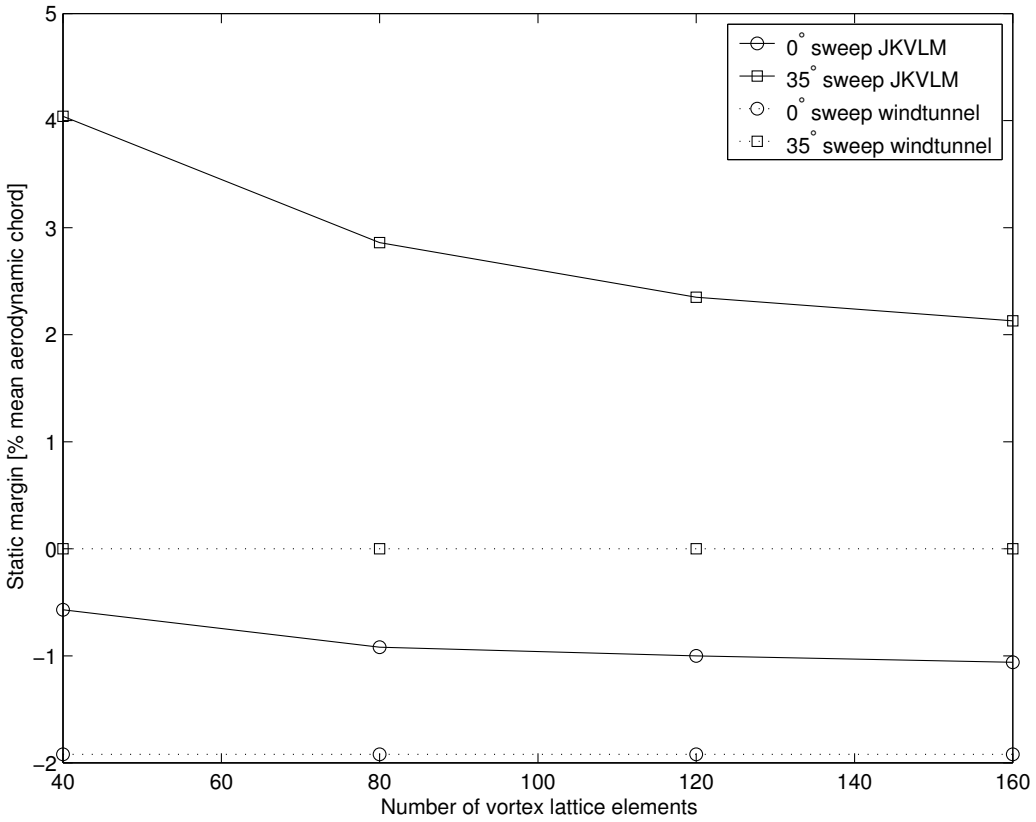

Figure G.1: Convergence of static margin with respect to number of VLM elements.

as the static margin for the test specimen. In the case of an aircraft, the CG of the aircraft would be used as this reference point. The comparison is presented in Table G.3. The following limitations of VLM's are important when making this comparison:

- Airfoil thickness is not modelled and this leads to the underestimation of aerodynamic lift in the case of very thick airfoil sections.
- JKVLM does not model wing camber. This leads to an incorrect estimate of the zero lift angle of attack.
- Viscous effects are neglected in VLM estimates.

- The VLM results are only valid in the linear region of aerodynamics and at small angles of attack (typically -5° to 5°). This is not a severe limitation for the current study since all simulations are with small disturbances and at small angles of attack.

Table G.3: Comparison of the wind tunnel and VLM results for the neutral point and static margin.

	JKVLM		Wind tunnel	
	Unswept wing	35° swept-back wing	Unswept wing	35° swept-back wing
Static margin	-1.06%	2.13%	-1.92%	0.00%
Neutral point	44.40%	125.03%	43.54%	122.90%

It may be concluded from the results presented in Table G.3 that JKVLM has a maximum error of around 3% for the estimation for the static margin at 30° sweep angles. The VLM tends to overestimate the magnitude of static margin. The prediction error becomes greater at higher wing sweep angles. The error in prediction at greater sweep angles may be ascribed to the fact that spanwise flow effects are not modelled. Viscous effects are also neglected and therefore lift and aerodynamic moment are predicted incorrectly. This in turns leads to incorrect neutral point and static margin estimates.

G.4 Conclusions

The prediction error of the neutral point (using VLM's) for unswept wings is less than 1% and less than 3% for swept wings. This should be viewed as sufficiently accurate for the purpose of a handling qualities investigation on a general configuration.

This level of accuracy is also sufficient for the case of the Exulans, since no complete design (or prototype aircraft) existed at the time of completion of this study. Possible future aerodynamic and fuselage shape design changes have the potential of changing the neutral point by a larger margin than

the error of the prediction method. Once the Exulans design is completed, the neutral point can be accurately estimated using methods such as CFD. The impact of any changes in neutral point may then be assessed by the sensitivity study presented in this document.

Furthermore it is possible to alter static margin within a limited range by changing aircraft CG. It should be possible to alter the CG of the Exulans by design changes within the 3% range.

Based on these points, the level of accuracy of the VLM is therefore judged to be acceptable for the purposes of this handling quality investigation.

Appendix H

Aircraft Configurations

The aircraft configurations listed in this section were used in the pitch control analysis simulations, as well as the gust response analysis simulations. The different configurations are described by means of codes. The legend of the codes is presented in the following table:

Legend for sweep symbols	
Symbol	Declaration
20°	20 degrees outboard wing sweep (γ)
24°	24 degrees outboard wing sweep (γ)
30°	30 degrees outboard wing sweep (γ)
36°	36 degrees outboard wing sweep (γ)

Legend for static margins	
Symbol	Declaration
2%	2% @ 30° sweep
5%	5% @ 30° sweep
10.7%	10.7% @ 30° sweep
15%	15% @ 30° sweep

Legend for control authority	
Symbol	Declaration
cm20	control baseline minus 20% ($C_{L_{\delta_e}}$ kept at the baseline and $C_{M_{\delta_e}}$ reduced by 20%)
cp20	control baseline plus 20% ($C_{L_{\delta_e}}$ kept at the baseline and $C_{M_{\delta_e}}$ increased by 20%)
c	control baseline

Legend for damping ratio	
Symbol	Declaration
dm20	damping baseline minus 20%
dp20	damping baseline plus 20%
d	damping baseline

The aircraft configurations presented in the following tables were used in the pitch control analysis simulations.

Table H.1: The aircraft configurations investigated in the pitch control effectiveness analysis.

Number	Description
1	20° 2% cm20 dm20
2	20° 2% cm20 dp20
3	20° 2% cm20 d
4	20° 2% cp20 dm20
5	20° 2% cp20 dp20
6	20° 2% cp20 d
7	20° 2% c dm20
8	20° 2% c dp20
9	20° 2% c d
10	20° 5% cm20 dm20
11	20° 5% cm20 dp20
12	20° 5% cm20 d
13	20° 5% cp20 dm20
14	20° 5% cp20 dp20
15	20° 5% cp20 d
16	20° 5% c dm20
17	20° 5% c dp20
18	20° 5% c d
19	20° 10.7% cm20 dm20
20	20° 10.7% cm20 dp20
21	20° 10.7% cm20 d
22	20° 10.7% cp20 dm20
23	20° 10.7% cp20 dp20
24	20° 10.7% cp20 d
25	20° 10.7% c dm20
26	20° 10.7% c dp20
27	20° 10.7% c d
28	20° 15% cm20 dm20
29	20° 15% cm20 dp20
30	20° 15% cm20 d
31	20° 15% cp20 dm20
32	20° 15% cp20 dp20
33	20° 15% cp20 d
34	20° 15% c dm20
35	20° 15% c dp20
36	20° 15% c d

Number	Description
37	24° 2% cm20 dm20
38	24° 2% cm20 dp20
39	24° 2% cm20 d
40	24° 2% cp20 dm20
41	24° 2% cp20 dp20
42	24° 2% cp20 d
43	24° 2% c dm20
44	24° 2% c dp20
45	24° 2% c d
46	24° 5% cm20 dm20
47	24° 5% cm20 dp20
48	24° 5% cm20 d
49	24° 5% cp20 dm20
50	24° 5% cp20 dp20
51	24° 5% cp20 d
52	24° 5% c dm20
53	24° 5% c dp20
54	24° 5% c d
55	24° 10.7% cm20 dm20
56	24° 10.7% cm20 dp20
57	24° 10.7% cm20 d
58	24° 10.7% cp20 dm20
59	24° 10.7% cp20 dp20
60	24° 10.7% cp20 d
61	24° 10.7% c dm20
62	24° 10.7% c dp20
63	24° 10.7% c d
64	24° 15% cm20 dm20
65	24° 15% cm20 dp20
66	24° 15% cm20 d
67	24° 15% cp20 dm20
68	24° 15% cp20 dp20
69	24° 15% cp20 d
70	24° 15% c dm20
71	24° 15% c dp20
72	24° 15% c d

Number	Description
73	30° 2% cm20 dm20
74	30° 2% cm20 dp20
75	30° 2% cm20 d
76	30° 2% cp20 dm20
77	30° 2% cp20 dp20
78	30° 2% cp20 d
79	30° 2% c dm20
80	30° 2% c dp20
81	30° 2% c d
82	30° 5% cm20 dm20
83	30° 5% cm20 dp20
84	30° 5% cm20 d
85	30° 5% cp20 dm20
86	30° 5% cp20 dp20
87	30° 5% cp20 d
88	30° 5% c dm20
89	30° 5% c dp20
90	30° 5% c d
91	30° 10.7% cm20 dm20
92	30° 10.7% cm20 dp20
93	30° 10.7% cm20 d
94	30° 10.7% cp20 dm20
95	30° 10.7% cp20 dp20
96	30° 10.7% cp20 d
97	30° 10.7% c dm20
98	30° 10.7% c dp20
99	30° 10.7% c d
100	30° 15% cm20 dm20
101	30° 15% cm20 dp20
102	30° 15% cm20 d
103	30° 15% cp20 dm20
104	30° 15% cp20 dp20
105	30° 15% cp20 d
106	30° 15% c dm20
107	30° 15% c dp20
108	30° 15% c d

Number	Description
109	36° 2% cm20 dm20
110	36° 2% cm20 dp20
111	36° 2% cm20 d
112	36° 2% cp20 dm20
113	36° 2% cp20 dp20
114	36° 2% cp20 d
115	36° 2% c dm20
116	36° 2% c dp20
117	36° 2% c d
118	36° 5% cm20 dm20
119	36° 5% cm20 dp20
120	36° 5% cm20 d
121	36° 5% cp20 dm20
122	36° 5% cp20 dp20
123	36° 5% cp20 d
124	36° 5% c dm20
125	36° 5% c dp20
126	36° 5% c d
127	36° 10.7% cm20 dm20
128	36° 10.7% cm20 dp20
129	36° 10.7% cm20 d
130	36° 10.7% cp20 dm20
131	36° 10.7% cp20 dp20
132	36° 10.7% cp20 d
133	36° 10.7% c dm20
134	36° 10.7% c dp20
135	36° 10.7% c d
136	36° 15% cm20 dm20
137	36° 15% cm20 dp20
138	36° 15% cm20 d
139	36° 15% cp20 dm20
140	36° 15% cp20 dp20
141	36° 15% cp20 d
142	36° 15% c dm20
143	36° 15% c dp20
144	36° 15% c d

The aircraft configurations presented in the following tables were used in the gust response analysis simulations.

Table H.2: The aircraft configurations investigated in the gust response and eigenvalue analysis.

Number	Description
1	20° 2% dm20
2	20° 2% dp20
3	20° 2% d
4	20° 5% dm20
5	20° 5% dp20
6	20° 5% d
7	20° 10.7% dm20
8	20° 10.7% dp20
9	20° 10.7% d
10	20° 15% dm20
11	20° 15% dp20
12	20° 15% d
13	24° 2% dm20
14	24° 2% dp20
15	24° 2% d
16	24° 5% dm20
17	24° 5% dp20
18	24° 5% d
19	24° 10.7% dm20
20	24° 10.7% dp20
21	24° 10.7% d
22	24° 15% dm20
23	24° 15% dp20
24	24° 15% d

Number	Description
25	30° 2% dm20
26	30° 2% dp20
27	30° 2% d
28	30° 5% dm20
29	30° 5% dp20
30	30° 5% d
31	30° 10.7% dm20
32	30° 10.7% dp20
33	30° 10.7% d
34	30° 15% dm20
35	30° 15% dp20
36	30° 15% d
37	36° 2% dm20
38	36° 2% dp20
39	36° 2% d
40	36° 5% dm20
41	36° 5% dp20
42	36° 5% d
43	36° 10.7% dm20
44	36° 10.7% dp20
45	36° 10.7% d
46	36° 15% dm20
47	36° 15% dp20
48	36° 15% d